

Epitaxial growth and electrical-transport properties of Ti(7)Si(2)C(5) thin films synthesized by reactive sputter-deposition

T H Scabarozi, J D Hettinger, S E Lofland, Jun Lu, Lars Hultman,
Jens Jensen and Per Eklund

Linköping University Post Print

N.B.: When citing this work, cite the original article.

Original Publication:

T H Scabarozi, J D Hettinger, S E Lofland, Jun Lu, Lars Hultman, Jens Jensen and Per Eklund, Epitaxial growth and electrical-transport properties of Ti(7)Si(2)C(5) thin films synthesized by reactive sputter-deposition, 2011, Scripta Materialia, (65), 9, 811-814.

<http://dx.doi.org/10.1016/j.scriptamat.2011.07.038>

Copyright: Elsevier

<http://www.elsevier.com/>

Postprint available at: Linköping University Electronic Press

<http://urn.kb.se/resolve?urn=urn:nbn:se:liu:diva-71773>

Accepted Manuscript

Epitaxial growth and electrical-transport properties of $\text{Ti}_7\text{Si}_2\text{C}_5$ thin films synthesized by reactive sputter-deposition

T.H. Scabarozi, J.D. Hettinger, S.E. Lofland, J. Lu, L. Hultman, J. Jensen, P. Eklund

PII: S1359-6462(11)00437-4

DOI: [10.1016/j.scriptamat.2011.07.038](https://doi.org/10.1016/j.scriptamat.2011.07.038)

Reference: SMM 8979

To appear in: *Scripta Materialia*

Received Date: 19 July 2011

Accepted Date: 24 July 2011

Please cite this article as: T.H. Scabarozi, J.D. Hettinger, S.E. Lofland, J. Lu, L. Hultman, J. Jensen, P. Eklund, Epitaxial growth and electrical-transport properties of $\text{Ti}_7\text{Si}_2\text{C}_5$ thin films synthesized by reactive sputter-deposition, *Scripta Materialia* (2011), doi: [10.1016/j.scriptamat.2011.07.038](https://doi.org/10.1016/j.scriptamat.2011.07.038)

This is a PDF file of an unedited manuscript that has been accepted for publication. As a service to our customers we are providing this early version of the manuscript. The manuscript will undergo copyediting, typesetting, and review of the resulting proof before it is published in its final form. Please note that during the production process errors may be discovered which could affect the content, and all legal disclaimers that apply to the journal pertain.



Epitaxial growth and electrical-transport properties of $\text{Ti}_7\text{Si}_2\text{C}_5$ thin films synthesized by reactive sputter-deposition

T. H. Scabarozzi^{1,2}, J. D. Hettinger¹, S. E. Lofland¹, J. Lu², L. Hultman², J. Jensen,²
P.Eklund^{2,*}

¹ Department of Physics and Astronomy, Rowan University, Glassboro, NJ 08028, USA

²Thin Film Physics Division, Department of Physics, Chemistry, and Biology, IFM,
Linköping University, SE-581 83 Linköping, Sweden

*Corresponding author. E-mail perek@ifm.liu.se

Abstract

Epitaxial predominantly phase-pure $\text{Ti}_7\text{Si}_2\text{C}_5$ thin films were grown onto $\text{Al}_2\text{O}_3(0001)$ by reactive magnetron sputtering. The c -axis lattice constant is ~ 60.2 Å; the $\text{Ti}_7\text{Si}_2\text{C}_5$ unit cell comprising alternating Ti_3SiC_2 -like and Ti_4SiC_3 -like half-unit-cell stacking repeated three times. Elastic recoil detection analysis showed a few percent of nitrogen in the films from the acetylene gas used. The nitrogen-induced stabilization mechanism for $\text{Ti}_7\text{Si}_2\text{C}_5$ relative to Ti_3SiC_2 and Ti_4SiC_3 is discussed. Electrical-transport measurements showed metallic temperature dependence and a room-temperature resistivity of ~ 45 $\mu\Omega\text{cm}$.

MAX phases are a group comprising ~60 ternary compounds with a general composition of $M_{n+1}AX_n$ ($n=1, 2, \text{ or } 3$) where M is a transition metal, A is an A-group element, and X is carbon or nitrogen [1,2,3]. Usually, the MAX phases are classified into three groups based on their n values, i.e., “211” for $n = 1$, “312” for $n = 2$, and “413” for $n = 3$. The archetypical $Ti_{n+1}SiC_n$ phases are in existing applications as ohmic contacts to SiC [4,5,6,7] and of potential interest in a range of other applications [2]. They have been synthesized in single crystal form as thin films [2] and very recently Ti_3SiC_2 bulk single crystals have been made [8,9]. Further, in the Ti-Si-C system, Palmquist et al. [10] first demonstrated the “intergrown structures” $Ti_5Si_2C_3$ and $Ti_7Si_2C_5$. These “523” and “725” phases comprise alternating layers of “211” and “312” or “312” and “413”, respectively. The same phases were also demonstrated in the Ti-Ge-C system [11]. Zhou et al. [12] later reported another “523” phase, $(V,Cr)_5Al_2C_3$. These compounds have only been observed as minority phases in samples consisting primarily of M_2AC and M_3AC_2 (for “523” phases) or M_3AC_2 and M_4AC_3 (for “725” phases). It has even been debated whether it is appropriate to describe them as *phases*, since they only existed in small quantities and never in macroscopic amounts. Here, we resolve this issue by synthesizing epitaxial virtually single-phase $Ti_7Si_2C_5$ thin films. Our results suggest a nitrogen-induced physical mechanism for the stabilization of this complex phase relative to a simple mixture of Ti_3SiC_2 and Ti_4SiC_3 .

$Ti_7Si_2C_5$ thin films were synthesized in a custom-built ultra-high vacuum magnetron sputtering chamber with an ultimate base pressure of 10^{-7} mbar [13]. Films were deposited at a substrate temperature of 850 °C (determined by optical pyrometer

and calibrated with a thermocouple) in a mixture of high-purity argon (99.999%) and industrial-grade acetylene (C_2H_2) gas at a total pressure of 2.7 Pa (20 mTorr). The argon flow was maintained at 40 sccm while the acetylene was varied from 3.5-4.0 sccm. Two 50-mm cathodes positioned directly over a rotating table contained the titanium (99.95%) and silicon (99.999%) targets. A direct current (DC) power source varied from 135-160 W was used for titanium while a radio frequency (RF) power source varied from 400-500 W was used on the silicon, yielding a deposition rate of ~ 1 - $1.2 \mu\text{m/h}$. The substrate rotation rate was approximately 18 rpm with a substrate-cathode distance of 10 cm. All depositions were performed on (0001)-oriented polished sapphire (Al_2O_3) wafers and were at floating potential. X-ray diffraction (XRD) was performed on a Panalytical Empyrean configured in standard θ - 2θ Bragg-Brentano geometry with $Cu-K_\alpha$ radiation. Electron microscopy was performed with a LEO 1530VP scanning electron microscope (SEM) and a FEI Tecnai G2 TF 20 UT field emission gun transmission electron microscopy (TEM) operated at 200 kV acceleration voltage. Cross sectional TEM samples were prepared by mechanical polishing down to a thickness of $\sim 50 \mu\text{m}$, and ion milling in a Gatan Precision Ion Polishing System (PIPS) with Ar ions with energy of 5 keV with a final polishing step with 2 keV Ar ions. Sample composition and thickness were measured with a Rigaku ZSX Primus II wavelength dispersive x-ray fluorescence (WDXRF) spectrometer with RhK_α radiation. Elemental depth profiles of as-deposited films were obtained from time-of-flight elastic recoil detection analysis (ToF-ERDA) with a 40 MeV $^{127}I^{9+}$ ion beam at Uppsala University [14]. The recoil angle was 45° while the incident angle of primary ions and the exit angle of recoils were both set to 67.5° relative to the surface normal. All spectra were analyzed using the CONTES code

[15] to obtain relative atomic concentration profiles from the recoil energy of each element. Electrical transport measurements were carried out on microbridges 400 μm wide and 1600 μm long. The bridges were defined by standard photolithographic techniques followed by a wet etch. The resistivity was measured as a function of temperature T for $2\text{ K} \leq T \leq 300\text{ K}$ range with a Quantum Design Physical Properties Measurement System (PPMS) by a four-probe technique. Details can be found elsewhere [16].

Figure 1 shows an X-ray diffractogram of a virtually phase-pure (000 ℓ)-oriented $\text{Ti}_7\text{Si}_2\text{C}_5$ thin film. The minute peaks not indexed in Fig. 1 originate from a very small amount of Ti_4SiC_3 ; no TiC or Ti_3SiC_2 can be detected. Figure 2 is a high-resolution TEM image showing the hexagonal layered structure with the “725” structure formed by interleaving half-unit-cell layers of “312” and “413”. From the XRD results, the c -axis lattice constant is determined to 60.2 \AA . Note that this refers to a unit cell with a c axis *three* times the average of the Ti_3SiC_2 and Ti_4SiC_3 unit cells. The description of $\text{Ti}_7\text{Si}_2\text{C}_5$ as alternating half-unit-cell layers of Ti_3SiC_2 and Ti_4SiC_3 repeated twice to form a “725” supercell is a good first approximation but not completely accurate as it would yield a c axis *twice* the average of Ti_3SiC_2 and Ti_4SiC_3 , i.e., the sum of the two c axes. Rather, the alternating stacking of even and odd numbers of Ti layers induces a lateral translation of the Si position in the lattice (c.f., Fig. 2), i.e., the Si atoms are not positioned above each other until after *three* repetitions [2,10]. The indexes of the 000 ℓ reflections in the θ -2 θ diffractogram (Fig. 1) are therefore $\ell=3n$ ($n=1, 2, 3\dots$).

Figure 3 shows the depth profile of composition as determined by ToF-ERDA. The composition is essentially constant with depth and is Ti:Si:C = 7:2:5 within the error bars of the measurement. However, most notable is the presence of nitrogen in the films. The source of the nitrogen is likely the acetylene, only being industrial grade. Ti-Si-C films (with Ti:Si:C = 7:2:5 composition) deposited from elemental targets of carbon, titanium, and silicon contained less than 0.3 at. % nitrogen as indicated by WDXRF (not shown). These films were not pure $\text{Ti}_7\text{Si}_2\text{C}_5$, but contained large amounts of Ti_3SiC_2 and/or Ti_4SiC_3 (not shown, very similar to films described in, e.g., Ref. 10). In contrast, deposits in acetylene showed 1.4-2.5 at. % nitrogen (confirmed by both ERDA and WDXRF).

Thus, both in the present work and previous work [10], deposition of Ti-Si-C films from elemental targets of carbon, titanium, and silicon (with Ti:Si:C = 7:2:5 composition) yield a $\text{Ti}_3\text{SiC}_2/\text{Ti}_4\text{SiC}_3$ phase-mixture with $\text{Ti}_7\text{Si}_2\text{C}_5$ as a minority phase; while the present reactively sputtered nitrogen-containing films are virtually phase-pure $\text{Ti}_7\text{Si}_2\text{C}_5$. The *c*-axis lattice parameter of ~ 60.2 Å is somewhat lower than the value of 60.62 Å suggested by Palmquist *et al.* [10] (again, referring to three times the average of the pure Ti_3SiC_2 and Ti_4SiC_3 unit cells). The effective stabilization of the $\text{Ti}_7\text{Si}_2\text{C}_5$ phase by the introduction of a few percent of nitrogen in the reactive gas might be explained by N hindering the known stable Ti_3SiC_2 and Ti_4SiC_3 from forming. The otherwise expected step-flow mechanism [2,7,10] may be intermittently blocked by N at surface steps (forming a tetrahedrally coordinated Si-N bond). Instead, a self-organizing process would

be operating with TiC_x slabs terminated by monolayers of segregating Si in a 413+312 repetitive manner corresponding to the set composition. Another possible explanation is that the N incorporation might offset the energy of the competing compounds in favor of the 725 phase. While this possibility can be tested by *ab initio* calculations (cf., e.g., Refs. 17,18), it is less likely as no Ti-Si-N MAX phases exist because of the preference for TiN and Si_3N_4 phase separation.

Figure 4 shows the electrical resistivity curves in the temperature range 2-300 K of $\text{Ti}_7\text{Si}_2\text{C}_5$ thin films along with Ti_3SiC_2 and Ti_4SiC_3 reference samples (the latter two grown from elemental targets of carbon, titanium and silicon). The room-temperature resistivity ρ of $\text{Ti}_7\text{Si}_2\text{C}_5$ of $\sim 45 \mu\Omega\text{cm}$ is intermediate between Ti_4SiC_3 ($\sim 67 \mu\Omega\text{cm}$) and Ti_3SiC_2 ($\sim 31 \mu\Omega\text{cm}$). The numbers for Ti_4SiC_3 and Ti_3SiC_2 are consistent with but systematically slightly higher than previously reported thin-film values [19]. The residual resistivity ratios (RRR, i.e., $\rho(300 \text{ K})/\rho(2 \text{ K})$) are 5.9 (Ti_3SiC_2) and 1.9 (Ti_4SiC_3) and 2.5 ($\text{Ti}_7\text{Si}_2\text{C}_5$). Since the residual resistivity ($\rho(2 \text{ K})$) depends on defect and impurity scattering, the RRR is indicative of sample quality and defects. It is therefore somewhat surprising that the RRR of $\text{Ti}_7\text{Si}_2\text{C}_5$ is higher than the Ti_4SiC_3 sample despite the incorporation of several percent of nitrogen; this fact indicates that the virtually phase-pure $\text{Ti}_7\text{Si}_2\text{C}_5$ is of high crystalline quality. The temperature coefficient of resistivity (TCR) of $\text{Ti}_7\text{Si}_2\text{C}_5$ is $\sim 0.1 \mu\Omega\text{cm/K}$; the same as for Ti_3SiC_2 . Note also that the TCR for Ti_3SiC_2 is slightly higher than the literature values of $\sim 0.08 \mu\Omega\text{cm/K}$ for bulk polycrystalline samples [20,21], suggesting some degree of anisotropy in electron-phonon coupling (cf., Ref. 22).

Variations in the relative composition of Ti and Si or in the Ar/acetylene ratio (results not shown) resulted in films containing $\text{Ti}_7\text{Si}_2\text{C}_5$, but with substantial fractions of Ti_3SiC_2 , Ti_4SiC_3 , and binary phases (TiC, Ti_5C_3). Thus, the process window with respect to reactive gas partial pressure for the synthesis of phase-pure $\text{Ti}_7\text{Si}_2\text{C}_5$ is relatively narrow, but apparently less sensitive than results for Ti_2AlN , which is the only previously reported MAX-phase synthesized by reactive sputtering in Ar/ N_2 [2]. In contrast, since the MAX-phase carbides can be easily grown by elemental- and compound-target sputter-deposition there has not been much interest in reactive deposition of carbide MAX phases until now. The present results show that it is time to reevaluate this opinion.

In conclusion, phase-pure $\text{Ti}_7\text{Si}_2\text{C}_5(0001)$ films have been fabricated by reactive sputter epitaxy and their electrical properties determined. The method is suitable to make large and complex inorganic crystal structures in a fast and inexpensive fashion. Our proposition of self-assembled nanolaminate crystals by segregation and monolayer precipitation of Si with a fourth element blocking lateral step-flow growth have far-reaching implications concerning the synthesis of compounds with any conceivable stacking order. Other yet more complex structures than the $\text{Ti}_7\text{Si}_2\text{C}_5$ phase can thus be envisioned.

Acknowledgments

Funding from the European Research Council, the Swedish Research Council, and the Swedish Foundation for Strategic Research is acknowledged. The WDXRF spectrometer

and the x-ray diffractometer were acquired by funding from NSF MRI grants 0821406 and 0960003.

References

- ¹ M. W. Barsoum, *Prog. Solid State Chem.* 28 (2000) 201.
- ² P. Eklund, M. Beckers, U. Jansson, H. Högberg, and L. Hultman, *Thin Solid Films* 518 (2010) 1851.
- ³ J.Y. Wang, Y.C. Zhou, *Annu. Rev. Mater. Res.* 39 (2009) 415.
- ⁴ Z. C. Wang, M. Saito, S. Tsukimoto, and Y. Ikuhara, *Adv. Mater.* 21 (2009) 4966.
- ⁵ Z. C. Wang, S. Tsukimoto, R. Sun, M. Saito, and Y. Ikuhara, *Appl. Phys. Lett.* 98 (2011) 104101.
- ⁶ K. Buchholt, R. Ghandi, M. Domeij, C.-M. Zetterling, J. Lu, P. Eklund, L. Hultman, and A. Lloyd Spetz *Appl. Phys. Lett.* 98 (2011) 042108.
- ⁷ K. Buchholt, P. Eklund, J. Jensen, J. Lu, A. Lloyd Spetz, and L. Hultman, *Scripta Mater.* 12 (2011) 1141.
- ⁸ F. Mercier, O. Chaix-Pluchery, T. Ouisse, and D. Chaussende, *Appl. Phys. Lett.* 98 (2011) 081912.
- ⁹ F. Mercier, T. Ouisse, and D. Chaussende, *Phys. Rev. B* 83 (2011) 075411.
- ¹⁰ J.-P. Palmquist, S. Li, P.O. Å. Persson, J. Emmerlich, O. Wilhelmsson, H. Högberg, M.I. Katsnelson, B. Johansson, R. Ahuja, O. Eriksson, L. Hultman, and U. Jansson, *Phys. Rev. B* 70 (2004) 165401.
- ¹¹ H. Högberg, P. Eklund, J. Emmerlich, J. Birch, and L. Hultman, *J. Mater. Res.* 20 (2005) 779.
- ¹² Y.C. Zhou, F. Meng, and J. Zhang, *J. Am. Ceram. Soc.* 91 (2008) 1357.
- ¹³ T. H. Scabarozzi, C. Gennaoui, J. Roche, T. Flemming, K. Wittenberger, P. Hann, B. Adamson, A. Rosenfeld, M. W. Barsoum, J. D. Hettinger, and S. E. Lofland *Appl. Phys. Lett.* 95 (2009) 101907.
- ¹⁴ H. J. Whitlow, G. Possnert, and C. S. Petersson, *Nucl. Instr. and Meth. B* 27 (1987) 448.
- ¹⁵ M. S. Janson, "CONTES, Conversion of Time-Energy Spectra, a program for ERDA data analysis," [unpublished manual, Uppsala University] (2004).
- ¹⁶ S.E. Lofland, J.D. Hettinger, T. Meehan, A. Bryan, P. Finkel, S. Gupta, M.W. Barsoum, G. Hug, *Phys. Rev. B* 74 (2006) 174501.
- ¹⁷ J. Rosén, P. O. Å. Persson, M. Ionescu, A. Kondyurin, D. R. McKenzie, and M. M. M. Bilek, *Appl. Phys. Lett.* 92 (2008) 064102.
- ¹⁸ J. Rosén, M. Dahlqvist, S. I. Simak, D. R. McKenzie, and M. M. M. Bilek, *Appl. Phys. Lett.* 97 (2010) 073103.
- ¹⁹ J. Emmerlich, P. Eklund, D. Rittrich, H. Högberg, L. Hultman, *J. Mater. Res.* 22 (2007) 2279.
- ²⁰ M. W. Barsoum, H.-I. Yoo, I. K. Polushina, V. Y. Rud', Y. V. Rud', and T. El-Raghy *Phys. Rev. B* 62 (2000) 10194.
- ²¹ P. Finkel, J. D. Hettinger, S. E. Lofland, M. W. Barsoum, and T. El-Raghy, *Phys. Rev. B* 65 (2001) 035113.
- ²² P. Eklund, M. Bugnet, V. Mauchamp, S. Dubois, C. Tromas, J. Jensen, L. Piraux, L. Gence, M. Jaouen, T. Cabioch, *Phys. Rev. B.* in press, 2011

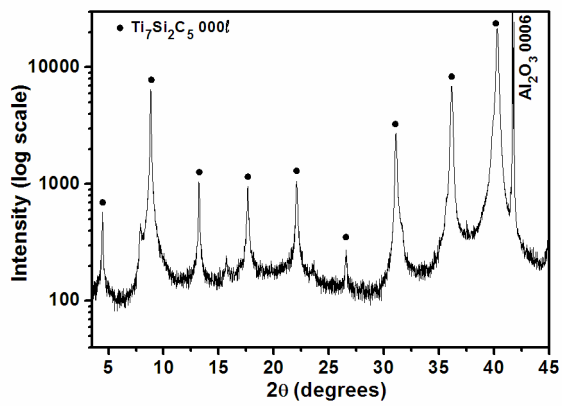
Figure Captions

Fig. 1 X-ray diffractogram of $\text{Ti}_7\text{Si}_2\text{C}_5$ thin films grown on $\text{Al}_2\text{O}_3(0001)$. The minute peaks not indexed in the figure originate from a very small amount of the secondary phase Ti_4SiC_3 .

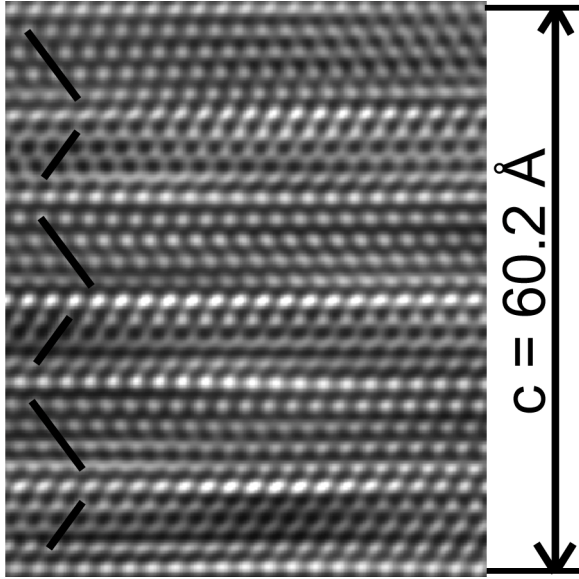
Fig. 2 High-resolution TEM image of $\text{Ti}_7\text{Si}_2\text{C}_5$ thin film; tilted bars in the left are guides for the eye indicating the alternating “312” and “413” stacking.

Fig. 3 ERDA depth profile of a phase-pure $\text{Ti}_7\text{Si}_2\text{C}_5$ thin film, showing no significant variation in composition with depth and a constant nitrogen content of $\sim 2\%$.

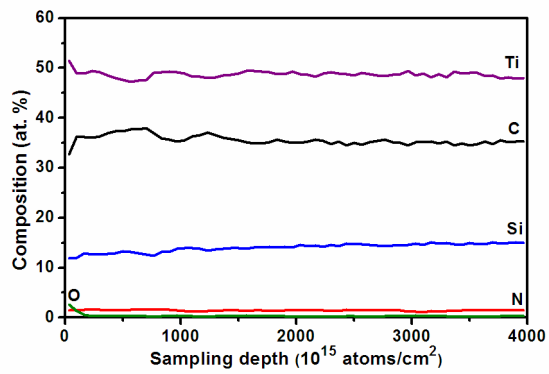
Fig. 4 Electrical resistivity of $\text{Ti}_7\text{Si}_2\text{C}_5$ in the temperature range 2-300 K along with Ti_3SiC_2 and Ti_4SiC_3 reference samples.



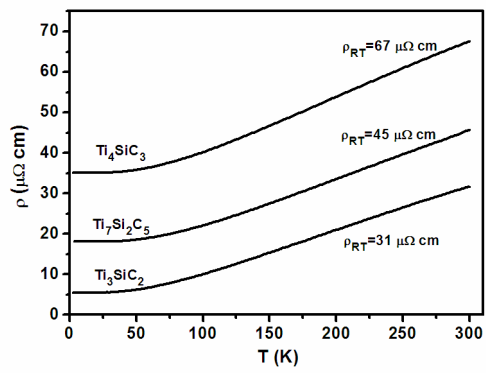
ACCEPTED MANUSCRIPT



ACCEPTED MANUSCRIPT



ACCEPTED MANUSCRIPT



ACCEPTED MANUSCRIPT